Electrofluidic Lipid Membrane Biosensor

*Young Kwang Lee and Jwa-Min Nam**

A host of significant biochemical processes such as materials transport, cellular signalling, and pathogenic pathways take place on cell membranes,[1] and over 50% of the 100 best-selling marketed drugs target membrane-associated proteins.[2] Correspondingly, there has been a growing demand for the development of highly sensitive biosensing platforms compatible with cellular membrane components, e.g., membrane receptors. Supported lipid bilayers (SLBs), which capture many important biological features of cell membranes, are a promising tool in this respect.[3] Recently, a wide variety of SLB-based systems to detect the binding of target proteins to membranes have been reported, e.g., colloidal particle phase transition,[4] electrochemical sensing,[5] quartz-crystal microbalance measurements,[6] nanowire/tube-field effect transistors,[7] planar/localized surface plasmon resonance,[8] and single-nanoparticle tracking.[9] However, these SLB techniques often require complicated and cumbersome experimental procedures, especially for high-throughput applications, and present a poor limit of detection (LOD) and limited dynamic range. In order to facillitate the widespread use of SLBs as biosensing and screening platforms, it is essential to improve assay sensitivity, reliability, and throughput. Further, assay complexity, quantification of targets, and assay cost and time are also issues that need to be addressed.

Electrical manipulation of charged species exhibits high reproducibility and compatibility with biomolecules. Therefore, this technique has been well developed, especially for sensing and separation of biochemical species.[10] It has also been applied over the past two decades to the quantitative study of electric field-induced spatial reorganization of charged membrane species in a confined section of supported membrane.[11] However, most of these works have focused on the separation of biomembrane species.[12] Herein, we used SLB electrophoresis to develop a patterned SLB-based electrofluidic (EF) biosensing method for a rapid, sensitive, and high-throughput detection of the cell membrane receptor-binding ligands in an array format (**Figure 1**). This EF membrane biosensor is inspired by the naturally occurring phenomenon on cell membranes in which ligand binding can affect overall membrane fluidity by coordinating organization of connected receptors and other signaling molecules

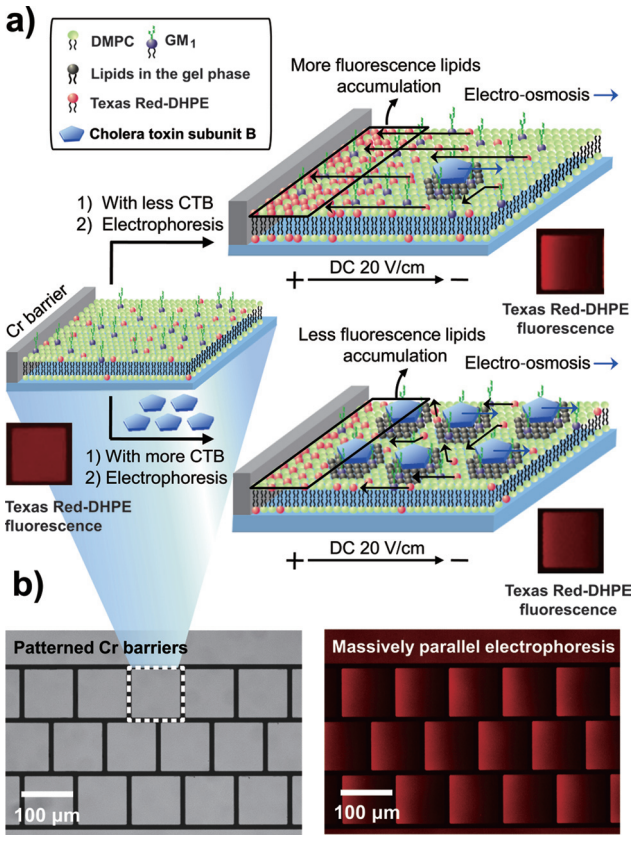

Figure 1. a) Schematic illustration of the electrofluidic lipid membrane biosensor. Red insets are epifluorescence microscope images of the SLB and each corresponds to the adjacent diagram. b) Left: Optical microscope image of multiple Cr corrals patterned on a glass substrate. The 100 µm × 100 µm corral lane is exclusively used in this study (see the Supporting Information for more details) and the single corral is highlighted with white dashed line. Right: Parallel and simultaneous electrophoresis of multiple SLB patterns.

for a corresponding cellular response.[1b,c,13] For target protein detection, we monitored the change in the lateral fluidity of the receptor-displaying SLB arising from target protein binding, in which detection signal was electrophoretically amplified with the EF lipid bilayer patterned on a glass substrate (Figure 1). Here, one can rapidly concentrate negatively charged, fluorescent lipids that do not participate in target recognition events onto a Cr barrier using an electric field. Electrical movement of membrane-incorporated, charged species is intrinsically circumstantial, and thus reflective of a stationary environment with different viscosity when proteins are bound.[12b,c] Our basic principle is that, when more target molecules are added and bound to lipids, these target-bound lipid domains become gel phase

Y. K. Lee, Prof. J.-M. Nam
Department of Chemistry
Seoul National University
599 Gwanak-ro, Gwanak-gu,
Seoul, 151-747, South Korea
E-mail: jmnam@snu.ac.kr

DOI: 10.1002/smll.201102093

small NANO MICRO

and act as obstacles that hinder the electrical movement of charged, fluorophore-modified lipids toward a Cr barrier (Figure 1a).[14] Importantly, under an electric field, electrical motion of fluorescent-probe lipids and membrane-bound targets are governed by two different drifting mechanisms, such as electrophoresis and electro-osmosis. The combination of electrophoresis and electro-osmosis makes probe lipids and target proteins drift in opposite directions from each other (Figure 1a). It further amplifies the decrease in electrical mobility of probe lipids, when target proteins are bound to the lipid surface, by providing more effective and frequent collisions with the drift obstacles. The electrophoresis and electro-osmosis-based dual amplification strategy on the patterned EF lipid bilayer allows for detection of the subtle reduction in the SLB fluidity, visualized as a lowering of the accumulation of fluorescent-probe lipids near the Cr barrier region. As a proof-of-concept experiment, the interactions between cholera toxin and lipid-tethered ganglioside GM_1 were monitored and quantified (Figure 1a). When lipid-tethered GM_1 molecules are bound with multivalent, cholera toxin subunit B (CTB), thermal motions of GM_1, a well-known lipid-raft marker, are significantly restricted and they are locally concentrated around the CTB. This gives rise to the reduction of lipid mobility due to long-range correlation in chain alignment of the neighboring lipids close to the binding site. These CTB-GM_1 complexes serve as seeds to nucleate gel-phase domains extending beyond the immediate binding sites in the SLB.[14] Further, the free diffusion of lipids in the deep fluid-phase region is hindered by the resulting gel domains that act as impermeable obstacles.[15] These suggest the CTB molecules bound on the SLB can affect lipid movement in both gel and fluid phases in different ways, and, consequently, whole lipid fluidity depends on CTB concentration and binding to the SLB. This membrane structure modulation by protein binding could be maximized at the phase transition temperature (T_m) of the nonbinding background lipids (T_m of 1,2-dimyristoyl-*sn*-glycero-3-phosphocholine (DMPC) = 23 °C) because of a minimum energy requirement to cause a phase transition from fluid to gel phases.[14] The consequent alteration in the CTB, concentration-dependent, gel-fluid coexistence regime, can be clearly differentiated by subjecting the patterned fluorescent SLB to an external electric field applied parallel to the plane of the bilayer (see the Experimental Section for more details). In our platform, by laterally concentrating charged, fluorophore-labeled lipids, i.e., in this case (Texas Red)–1,2-dihexadecanoyl-*sn*-glycero-3-phosphoethanolamine (Texas Red–DHPE), one could rapidly detect membrane receptor-bound proteins. Here, the Cr barrier stops and concentrates the charged, fluorescent lipids, and the accumulated fluorescent lipids are quantified by an epifluorescence microscope (Figure 1a).

In a typical experiment, first a lipid bilayer composed of 99.3 mol% of DMPC, 0.5 mol% of GM_1 ganglioside and 0.2 mol% of negatively charged Texas Red–DHPE was deposited on a glass surface partitioned by 100 μm × 100 μm Cr corrals. Next, the substrate was loaded on an electrophoresis chamber filled with deionized (DI) water. Following the addition of target molecules (CTB in this case) and incubation at 25 °C for 30 min on an orbital shaker, the EF membrane sensor was operated at 23 °C (see the Experimental Section for more details). The flow of Texas Red–DHPE lipids toward a positive electrode was generated by applying voltage (DC 20 V cm^{-1}). Under the harsh electrophoresis condition, biomolecules such as proteins could be denatured by dramatic changes in pH and temperature.[16] To avoid this, we employed a relatively low voltage, and assay solutions with very low salt concentration (from nM to low μM). Typical currents in our platform were around 30 μA and this corresponds to a total power dissipation of 6×10^{-4} W, which should produce a negligible amount of Joule heating. Indeed, we did not observe temperature and pH change of electrophoresis solution by water electrolysis. Using this mild electrophoresis condition, the lipids accumulated against the Cr barrier (Figure 1a) and this accumulation results in a fluorescence gradient with a steep increase of fluorescence intensity toward the Cr barrier as a function of electrophoresis time (**Figure 2**a). After forcing the flow of Texas Red–DHPE, we measured the concentrated fluorescence intensity within a defined region (30 μm × 100 μm) in the immediate vicinity of the Cr barrier after electrophoresis (5 min in a typical case). The boxed region in Figure 2a shows the defined area. The accumulated fluorescence intensity (*AFI*) is defined by Equation (1):

$$AFI(t) = a\,S(t)/S(0) \quad (1)$$

where $S(t)$ is the fluorescence intensity summation inside a 30 μm × 100 μm region next to the Cr barrier (the area within the green box in Figure 2a) at time, t (min), of electrophoresis; $S(0)$ represents the fluorescence intensity summation before electrophoresis (the area within the white box in Figure 2a); and a is an arbitrary constant for normalization. The *AFI* values are the mean values measured from six individual corrals. Electrically driven fluorophore distribution is found to be nearly identical in all the corrals (Figures 1b and 2a). To test the reproducibility and reliability of this SLB platform, we repeatedly applied and released an electric field, and the *AFI* was measured from each corral (Figure 2b). The CTB-free SLB was electrophoresized at 20 V cm^{-1} for 5 min, then was left without an external electric field to completely relax back to uniformity. This process typically takes about

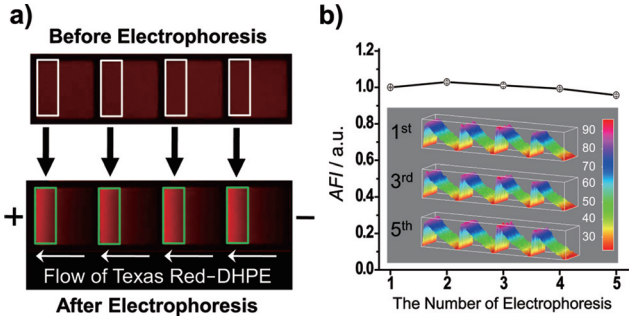

Figure 2. a) Typical epifluorescence microscope images of the patterned, electrofluidic SLB before and after electrophoresis. b) Results of reproducibility test. Accumulated fluorescence intensity (*AFI*) values during the five electrophoresis-recovery cycles were plotted. Inset profiles represent fluorescence distribution of four SLB patches used for quantitative analysis.

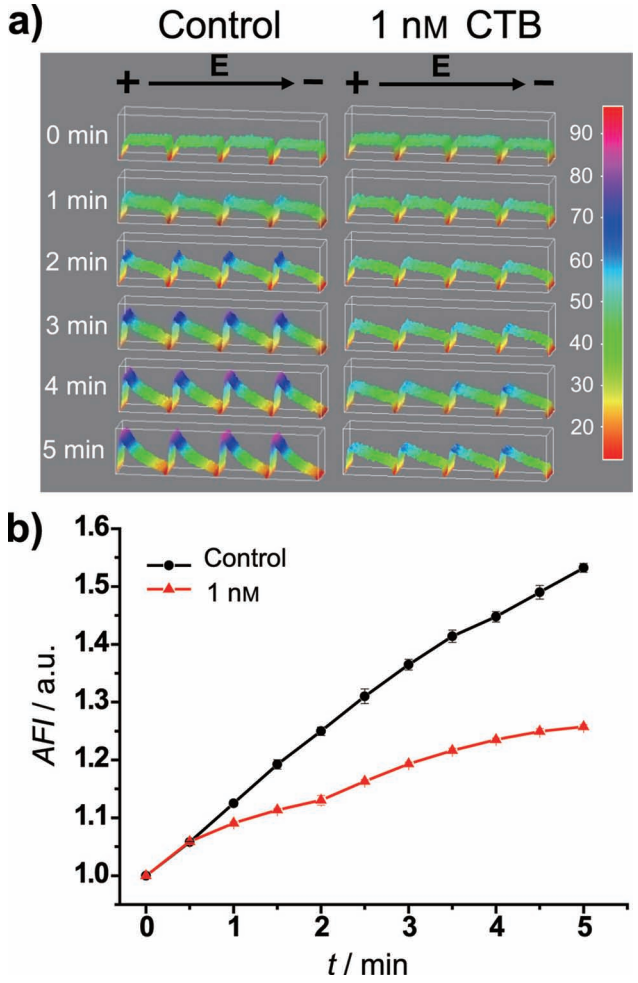

Figure 3. Time-dependent EF assay results. a) Surface profile plots of SLB fluorescence intensities without CTB (left) and with 1 nM CTB (right) under the influence of a DC voltage of 20 V cm^{-1}. The positive and negative electrodes were positioned on the left and right side of the frame, respectively. b) Accumulated fluorescent intensity (*AFI*) plot as a function of time.

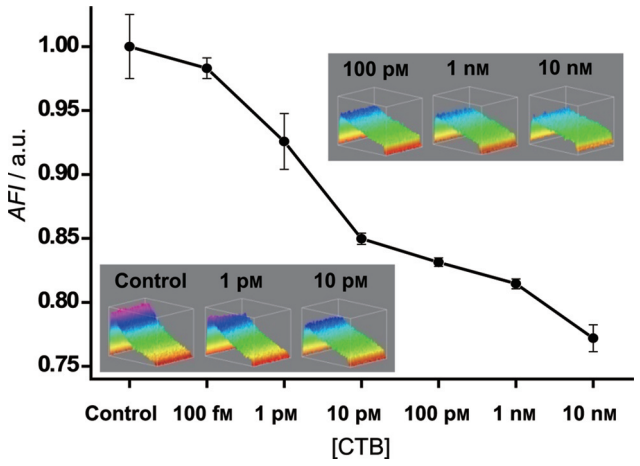

Figure 4. Electrically accumulated fluorescence intensity (*AFI*) plots as a function of CTB concentration. Insets are fluorescence surface plots of the EF membranes treated with various CTB concentrations. These images were used for quantitative examination. Here, Texas Red–DHPE lipids were concentrated for 5 min by an externally applied DC voltage of 20 V.

30 min. Remarkably, the results were nearly the same even after repeating this process five times (Figure 2b; standard deviation = 0.025). The results imply not only high assay reliability, but also low assay cost and time. Further, through the use of the same EF membrane lane repetitively, defect densities of the bilayer, that could vary from batch to batch, can be kept constant. This removes any possibility that the rate of electrophoresis is affected by the SLB quality rather than protein binding-induced phase transition.

To study electrophoresis time-dependence and determine appropriate electrophoresis time for an assay, a 1 nM CTB target solution was used as a model system (**Figure 3**). It is clear that the *AFI* was much lower when 1 nM CTB was treated than when no CTB was treated (Figure 3a). The plot of *AFI* value as a function of electrophoresis time shows that the results are time-dependent, and there is clear difference between the control and 1 nM CTB-added assay results (Figure 3b). The overall trend is that the difference widens as electrophoresis time increases. The protein binding-modulated electrofluidity change between two conditions could be distinguished from each other after >1 min of electrophoresis. Although it was confirmed that the fluorescence gradient undergoes no further changes and is saturated after 10 min electrophoresis for the target-free SLB, electrophoresis was conducted for only 5 min to avoid irreversible damage caused by prolonged exposure of the SLB, and other biochemical species, to an electric field.[11b,16] These results suggest that electrophoresis time is an important parameter in controlling detection signal and range.[10a]

The EF assay was then examined for its detection limit and dynamic range. The EF membrane bilayer was incubated with a detection target (CTB in this case) ranging from 100 fM to 10 nM for 30 min. The electrofluidity decreased as the amount of target increased, and the *AFI* is inversely proportional to the amount of added targets (**Figure 4**). Although 100 fM results could be differentiated from control results in average value comparison, the clear detection limit is 1 pM without assay optimization. The quantitative dynamic range for this assay was from 1 pM to 10 nM CTB concentration range. When these results were compared with other optical analysis techniques based on target-binding-induced lipid fluidity change, such as single-nanoparticle tracking, fluorescence correlation spectroscopy, and fluorescence recovery after photobleaching,[9,13b,14] the detection limit obtained with this EF biosensing platform is over ten-fold better for the same target. This could be ascribed to an active amplification step in which the electrophoresis enables more frequent and effective collisons between the probe lipids and the CTB-induced gel domains by locally concentrating probe lipids in the detection area (near the Cr barrier) and forcing the CTB-GM_1 complexes to be concentrated in the opposite direction to the probe lipids (**Figure 5**a). Indeed, when we used FITC-labeled CTB, instead of unlabeled CTB, for monitoring electrophoretic behavior of lipid-bound CTB, we observed the accumulation of CTB on the negative electrode side of the Cr corrals (Figure 5b). This means the drift of the CTB-GM_1 complexes is not governed by electrophoresis.

NANO MICRO small

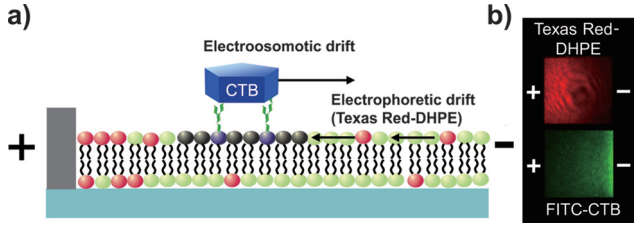

Figure 5. a) Schematic illustration of electrical motion of the CTB-GM_1 complexes and the negatively charged probe lipids under the influence of an electric field. b) Total internal reflection fluorescence microscope image of Texas Red-DHPE and FITC-labeled CTB after 5 min of exposure to a DC voltage of 20 V.

The CTB molecules are negatively charged, but they drift toward the negative electrode due to frictional coupling with electro-osmotic flows, i.e., where the electric field drives a bulk flow of cations near the negatively charged surface. This phenomenon has been previously reported in other protein-modified SLB systems.[11c,17] This electro-osmosis-generated counter-flow of lipid-tethered target proteins interferes with the electrophoretic accumulation of the probe lipids, and thus further widens the difference in the *AFI* values between target-free and target-bound samples.

Electro-osmotic flow can directly affect the field-induced motion of charged lipids by frictional coupling. It is known that a bulk electro-osmotic flow towards the cathode reduces the drift velocity of the negatively charged probe lipids and it is influenced by the surface charge.[11b–d] In our case, there is a possibility for electro-osmosis to be altered as the membrane surface is occupied by different numbers of charged target proteins. To examine this, we compared the zeta potentials of the lipid membrane before and after addition of 1 nM CTB. Silica microparticles (1 μm in diameter) were used as a solid support instead of a glass substrate to circumvent the exposure of lipid membrane to the air during the measurement. It was found that binding of CTB does not affect the zeta potential of the supported membrane (Figure S2, Supporting Information). This suggests that the electro-osmotic flow should not be altered by adding a different amount of CTB. Therefore, a scenario where reduction in the probe lipid mobility could be attributed to direct coupling of charged protein binding-modulated electro-osmotic flow can be excluded in our case.

The performence of the EF membrane sensor can largely depend on lipid composition. We performed an identical set of experiments with 1,2-dimyristoleoyl-*sn*-glycero-3-phosphocholine (DMOPC). Since the phase transition temperature of DMOPC is approximately –65 °C, the DMOPC membrane is in a fully disordered, liquid phase at operating temperature. The reduction in drift velocity of the lipid probe in the DMOPC membrane is much less than that in the DMPC membrane (Figure S3, Supporting Information). Protein binding gives rise to only marginal change in lipid motion for highly fluid DMOPC membranes. It shows a good agreement with previously reported results and provides evidence that the major mechanism of the EF sensor is based on protein binding-induced lipid ordering and consequent reduction in the long-range lateral mobility of membrane components, a phenomenon which frequently occurs in Nature.[14]

In summary, we have shown the first example of using the SLB array as an electrofluidic biosensing platform and working principles for this assay were proposed and validated. The assay sensitivity was ~1 pM, which is over ten-fold better than any other existing SLB fluidity-based detection methods for the same target, and the dynamic range was at least four orders of magnitude without optimization. The assay results were highly reliable and reproducible and can be applied to many corrals parallelly and simultaneously. Working-assay principles were also validated, and these included: electrophoresis-based lipid manipulation, target-binding-based phase transition in the SLB, the relationship between target-binding-induced gel domain and target quantification, and lipid-tethered protein electro-osmosis. This EF biosensing platform offers high reproducibility and reusability along with high sensitivity and a straightforward detection protocol for membrane-related targets of interest. Although this platform has been developed and is beneficial for exploring membrane-related receptor–ligand interactions, the EF membrane biosensor could also be used for probing other molecular interactions, as long as the receptor molecules could be tethered to the SLB.[14] Finally, our sensing platform, which mainly consists of a lipid bilayer on the metal-patterned substrate, can be miniaturized and integrated, via conventional microfluidic techniques, onto a single chip with a number of working stages; therefore, providing a device which could be beneficial in large-scale parallel screening and diagnostic applications.

Experimental Section

Materials: DMPC, DMOPC, and GM_1 ganglioside (Brain, Ovine-Ammonium Salt) were obtained from Avanti Polar Lipids (Alabaster, AL). Texas Red–DHPE triethylammonium salt was purchased from Molecular Probes (Eugene, OR). Pure CTB and FITC-modified CTB were purchased from Sigma-Aldrich (St. Louis, MO). Phosphate-buffered saline (PBS) solution was prepared by dissolving a PBS tablet (Sigma-Aldrich, St. Louis, MO) in 200 mL DI water, yielding 10 mM phosphate buffer solution with 2.7 mM potassium chloride and 137 mM sodium chloride (pH 7.4). Nanopure water with the minimum resistance (>18 MΩ cm^{-1}) was used in all the experiments. For vesicle preparation (vesicle extrusion), polycarbonate (PC) filters (Whatman, Fisher Scientific) with a pore diameter of 100 nm were used. Eagle 2000 glass substrate (Samsung Corning Co. Ltd., South Korea) was employed as a support for the lipid bilayer. Organic solvents such as chloroform, acetone and ethanol were obtained from Duksan Pure Chemicals Co. Ltd. (Kyeongi-do, South Korea). Sulfuric acid and hydrogen peroxide were purchased from Daejung Chemicals & Metals Co. Ltd. (Kyeongi-do, South Korea). To pattern Cr grid lines, AZ1512 positive photoresist and AZ300 MIF DEVELOPER (Clariant Co.) were used and Cr metal chips with a purity of 99.996% (Alfa Aesar, Ward Hill, MA) were used.

Fabrication of Cr Corrals on Glass Substrates: Cr corrals that function as a barrier to thermal diffusion and electrical drift of lipids in the supported lipid bilayer (SLB) were patterned on the surface of a glass substrate by photolithography and a subsequent

Cr lift-off process. For patterning, a glass substrate was cleaned by sonicating for 5 min in chloroform, acetone and ethanol. After each sonication step, the substrate was dried under a stream of nitrogen. Next, the substrate was etched by piranha solution, i.e., a 3:1 mixture of concentrated sulfuric acid and hydrogen peroxide, for 30 min and then rinsed thoroughly with DI water. AZ1512 positive photoresist (PR) was spun on the precleaned glass substrate at 4000 rpm for 35 s. The PR film-coated substrate was baked at 95 °C for 90 s to remove organic solvents. Light energy with an exposure dose of 500 mJ cm^{-2} was applied to the PR through a film photomask. The exposed area of the PR film was developed in AZ300 MIF DEVELPOER for 90 s, resulting in exposure of the glass surface in the desired PR pattern. Following photolithography, the PR-patterned substrate was loaded onto a thermal evaporator. A 10 nm-thick Cr film was thermally evaporated after the chamber pressure was lowered below 7.0×10^{-6} Torr. For revealing Cr patterns, the residual PR film was removed by sonicating in acetone for 10 min.

Formation of Supported Lipid Bilayers on Cr Grid Line-Patterned Glass Substrates: SLB was formed on a Cr-patterned glass substrate by the fusion of small unilamellar vesicles (SUVs). SUVs that are used in protein-sensing applications contain 99.3 mol% of DMPC, 0.5 mol% of GM_1, and 0.2 mol% of Texas Red–DHPE. The SUV solution was prepared by dissolving the appropriate amounts of lipids in chloroform. The lipid solution was evaporated in a 50 mL round-bottomed flask using a rotary evaporator at 50 °C, under vacuum, for 20 min. The lipid film was then further evacuated at room temperature for at least 4 h. The dried mixture was resuspended in DI water and hydrated overnight at 4 °C. The total lipid concentration was 2 mg mL^{-1}. The solution was extruded more than 11 times through a PC membrane with a pore diameter of 100 nm at 25 °C. The resulting SUV solution was mixed 3:1 v/v with PBS. The diluted solution (~50 μL) was dropped onto a plastic petri dish, and the prepatterned glass substrate etched with piranha solution was placed on top of the SUV solution. After 45 min of incubation at 25 °C, excess and unfused SUVs were eliminated from the surface of the substrate by rinsing with copious amounts of water.

Electrophoresis of Supported Lipid Bilayers: Cr barrier-patterned glass substrates coated with lipid bilayers were loaded onto a custom-built electrophoresis chamber (live cell instrument, Seoul, South Korea), as shown in Figure S1 of the Supporting Information. The substrate loading was carried out while keeping the substrate and chamber immersed in DI water. After loading the substrate, 20 V cm^{-1} of DC potential was applied parallel to the plane of the bilayer from two Pt electrodes that were placed on both sides of the chamber. Electrophoresis was conducted for 5 min at 23 °C. During the electrophoresis, the movement of Texas Red–DHPE was monitored by a Carl Zeiss Axiovert 200 inverted epifluorescence microscope (Carl Zeiss, Germany) with a 10× objective lens, and currents was measured by a Keithley 2400 SourceMeter (Keithley, USA). In order to perform the protein assay, the CTB-free SLB was first loaded onto the electrophoresis chamber and was electrophoresized as a negative control standard. This was conducted at 23 °C for 5 min under a DC voltage of 20 V cm^{-1}. After allowing the probe lipids to relax back to uniformity without the presence of an electric field, the target CTB solution was incubated at 25 °C for 30 min and electrophoresized again. This process was repeated with increasing CTB concentration. The total internal reflection fluorescence (TIRF) microscope image shown in Figure 5b was obtained with a Nikon TE-2000 microscope (Nikon, Japan). A 488 and 532 nm laser was introduced to a sample in a TIRF mode to excite FITC conjugated with CTB and Texas Red–DHPE for viewing through a 60× TIRF lens (NA 1.49). The emissions of FITC-CTB and Texas Red–DHPE were detected by a 500–530 nm band-pass filter and 590 nm long-pass filter, respectively.

Measurement of Zeta Potentials: In the zeta potential measurement, the SLB was deposited on the 1 μm silica beads (microParticles GmbH, Germany). Initially an equal volume of SUV solution, PBS and silica beads (0.5 mg mL^{-1}) were mixed and incubated for 45 min at 25 °C. Excess SUVs were then removed by centrifugation and redispersion with DI water three times. After incubation of 1 nM CTB for 30 min, zeta potential was measured with Zetasizer Nano ZS90 (Malvern Instruments Ltd., United Kingdom).

Supporting Information

Supporting Information is available from the Wiley Online Library or from the author.

Acknowledgements

This work was supported by the National Research Foundation of Korea (NRF) grant funded by the Korean government (MEST) (No. 2011-0018198); the 21C Frontier Functional Proteomics Project (FPR08-A2-150) through the National Research Foundation of Korea (NRF) from the Ministry of Education, Science and Technology; and the Industrial Core Technology Development Program of the Ministry of Knowledge Economy (No. 10033477). Y.K.L. was supported by the Seoul Science Fellowship Program of Seoul City, Korea.

[1] a) A. Miyazawa, Y. Fujiyoshi, N. Unwin, *Nature* **2003**, *423*, 949; b) D. M. Rosenbaum, S. G. F. Rasmussen, B. K. Kobilka, *Nature* **2009**, *459*, 356; c) D. Lingwood, K. Simons, *Science* **2009**, *327*, 46; d) H. Bayley, *Nature* **2009**, *459*, 651.

[2] a) J. Drews, *Science* **2000**, *287*, 1960; b) M. A. Yildirim, K.-I. Goh, M. E. Cusick, A.-L. Barabási, M. Vidal, *Nat. Biotechnol.* **2007**, *25*, 1119.

[3] a) M. Tanaka, E. Sackmann, *Nature* **2005**, *437*, 656; b) E. T. Castellana, P. S. Cremer, *Surf. Sci. Rep.* **2006**, *61*, 429; c) F. Giess, M. G. Friedrich, J. Heberle, R. L. Naumann, W. Knoll, *Biophys. J.* **2004**, *87*, 3213; d) Y.-H. M. Chan, S. G. Boxer, *Curr. Opin. Chem. Biol.* **2007**, *11*, 581.

[4] a) M. M. Baksh, M. Jaros, J. T. Groves, *Nature* **2004**, *427*, 139; b) E. M. Winter, J. T. Groves, *Anal. Chem.* **2006**, *78*, 174.

[5] a) S. Terrettaz, W.-P. Ulrich, R. Guerrini, A. Verdini, H. Vogel, *Angew. Chem. Int. Ed.* **2001**, *40*, 1740; b) Z. Wang, T. Wilkop, Q. Cheng, *Langmuir* **2005**, *21*, 10292; c) R. Naumann, A. Jonczyk, R. Kopp, J. van Esch, H. Ringsdorf, W. Knoll, P. Gräber, *Angew. Chem. Int. Ed.* **1995**, *34*, 2056; d) W. Römer, Y. H. Lam, D. Fischer, A. Watts, W. B. Fischer, P. Göring, R. B. Wehrspohn, U. Gösele, C. Steinem, *J. Am. Chem. Soc.* **2004**, *126*, 16267.

[6] a) C. Larsson, H. Bramfeldt, C. Wingren, C. Borrebaeck, F. Höök, *Anal. Biochem.* **2005**, *345*, 72; b) A. Janshoff, H.-J. Galla, C. Steinem, *Angew. Chem. Int. Ed.* **2000**, *39*, 4004.

[7] a) J. A. Martinez, N. Misra, Y. Wang, P. Stroeve, C. P. Grigoropoulos, A. Noy, *Nano Lett.* **2009**, *9*, 1121; b) X. Zhou, J. M. M.-Mirabal, H. G. Craighead, P. L. McEuen, *Nat. Nanotechnol.* **2007**, *2*, 185.
[8] a) C. L. Baciu, J. Becker, A. Janshoff, C. Sönnichsen, *Nano Lett.* **2008**, *8*, 1724; b) A. Dahlin, M. Zäch, T. Rindzevicius, M. Käll, D. S. Sutherland, F. Höök, *J. Am. Chem. Soc.* **2005**, *127*, 5043.
[9] Y.-H. Yang, J.-M. Nam, *Anal. Chem.* **2009**, *81*, 2564.
[10] a) M. Ammam, J. Fransaer, *Biosens. Bioelectron.* **2009**, *25*, 191; b) R. M. Brena, H. Auer, K. Kornacker, C. Plass, *Nat. Protoc.* **2006**, *1*, 52; c) J. Han, H. G. Craighead, *Science* **2000**, *288*, 1026.
[11] a) J. T. Groves, S. G. Boxer, H. M. McConnell, *J. Phys. Chem. B* **2000**, *104*, 119; b) J. T. Groves, S. G. Boxer, *Biophys. J.* **1995**, *69*, 1972; c) M. Tanaka, J. Hermann, I. Haase, M. Fischer, S.G. Boxer, *Langmuir* **2007**, *23*, 5638; d) C. Y.-Ishii, S. G. Boxer, *Langmuir* **2006**, *22*, 2384.
[12] a) L. Kam, S. G. Boxer, *Langmuir* **2003**, *19*, 1624; b) S. Daniel, A. J. Diaz, K. M. Martinez, B. J. Bench, F. Albertorio, P. S. Cremer, *J. Am. Chem. Soc.* **2007**, *129*, 8072; c) K. Suzuki, K. Hosokawa, M. Maeda, *J. Am. Chem. Soc.* **2008**, *130*, 1542.
[13] a) K. D. Mossman, G. Campi, J. T. Groves, M. L. Dustin, *Science* **2005**, *310*, 1191; b) V. Yamazaki, O. Sirenko, R. J. Schafer, J. T. Groves, *J. Am. Chem. Soc.* **2005**, *127*, 2826.
[14] M. B. Forstner, C. K. Yee, A. N. Parikh, J. T. Groves, *J. Am. Chem. Soc.* **2006**, *128*, 15221.
[15] a) T. V. Ratto, M. L. Longo, *Biophys. J.* **2002**, *83*, 3380; b) A. R. Burns, D. J. Frankel, T. Buranda, *Biophys. J.* **2005**, *89*, 1081.
[16] M. Ammam, J. Fransaer, *Electroanalysis* **2011**, *23*, 755.
[17] J. T. Groves, C. Wülfing, S. G. Boxer, *Biophys. J.* **1996**, *71*, 2176.

Received: October 5, 2011
Published online: January 23, 2012